Chemical Physics Letters 683 (2017) 478–482

Contents lists available at ScienceDirect

Chemical Physics Letters

journal homepage: www.elsevier.com/locate/cplett

Research paper

Solvation dynamics in water confined within layered manganese dioxide

Richard C. Remsing *, Michael L. Klein

Institute for Computational Molecular Science, Department of Chemistry, and Center for the Computational Design of Functional Layered Materials, Temple University, Philadelphia, PA 19122, United States

ARTICLE INFO

Article history:
Received 30 December 2016
In final form 27 February 2017
Available online 1 March 2017

Keywords:
Birnessite
Collective dynamics
Confinement
Solvent relaxation

ABSTRACT

The confined environment presented by layered transition metal oxides is conducive to a variety of chemical reactions. Despite intense interest in these materials, little is known regarding the microscopic details relevant to their catalytic activity. We characterize aspects of the dynamics governing a redox reaction in the interlayer environment between manganese dioxide sheets. The nonequilibrium solvation dynamics surrounding charge transfer between an ion and the surface are highly non-linear and exhibit long-time relaxation that is governed by collective dynamics. These dynamics are rationalized in terms of structural rearrangements, allowing connections to be made to more complex reactions in these materials.

1. Introduction

Layered manganese dioxides, known as birnessites, hold promise as water oxidation catalysts [1–4]. Between the two-dimensional MnO_2 layers of birnessite is a highly confined, single layer of water and cations [5–7], and this unique confined environment is conducive to redox chemistry. However, little information is known about the microscopic structure and dynamics surrounding reactivity in the highly confined interlayer region, illustrated in Fig. 1.

We recently reported an investigation of the structure in the interlayer solution [8]. In particular, we uncovered unique ion hydration structures resulting from a competition between water-water, water-surface, and water-ion interactions. The confined water acts as a two-dimensional fluid of dipoles, and cations typically share hydration shells due to a high concentration of ions in the interlayer (roughly 3:1 water:cation), qualitatively evidenced by the snapshot shown in Fig. 1. Water molecules shared between cations are frustrated, in the classic sense that they cannot adopt a unique orientation that minimizes their energy.

The appearance of frustrated hydration in two-dimensional confinement has a profound effect on the thermodynamics of charge transfer between ions and the surface [8]. Frustration enhances fluctuations of water molecules that are relevant to charge transfer, leading to non-Gaussian free energy landscapes. This non-Gaussian nature lowers the free energetic barrier for charge transfer beyond expectations from Marcus theory, which predicts parabolic free energy landscapes [9]. An increase in charge transfer rates accompanies the lowering of this barrier.

In order to understand chemical reactions like electron transfer, especially in unique environments like that presented by confinement within layered manganese dioxides, one needs to move beyond the static, equilibrium picture provided by thermodynamic calculations. In particular, solvent dynamics can significantly impact the nature of chemical reactivity [10–15]. Moreover, such dynamics can also significantly impact our understanding of multi-step chemical processes involving electron transfer reactions.

In this work we examine the dynamics of solvation surrounding electron transfer reactions involving hydrated cations confined between layered manganese dioxide sheets. Solvation dynamics can be significantly influenced by confinement effects [16–20] and nearby interfaces [17,21–28]. The existence of an underlying non-Gaussian free energy landscape [8] leads to violations of linear response theory in the non-equilibrium relaxation following a charge transfer event. These non-linear features originate in frustrated ion hydration structures, and the complex relaxation process can be rationalized in terms of local structural relaxation of water molecules in the hydration shell of the charge transfer site. We also detail the existence of long relaxation times — on the order of ns — which are governed by collective dynamics that control translational diffusion within the interlayer. We then conclude with a discussion of how understanding the origins of such long relaxation times may impact the study of step-wise reaction mechanisms involving charge transfer in similar environments.

* Corresponding author.
E-mail addresses: rremsing@temple.edu (R.C. Remsing), mlklein@temple.edu (M.L. Klein).

http://dx.doi.org/10.1016/j.cplett.2017.02.082
0009-2614/

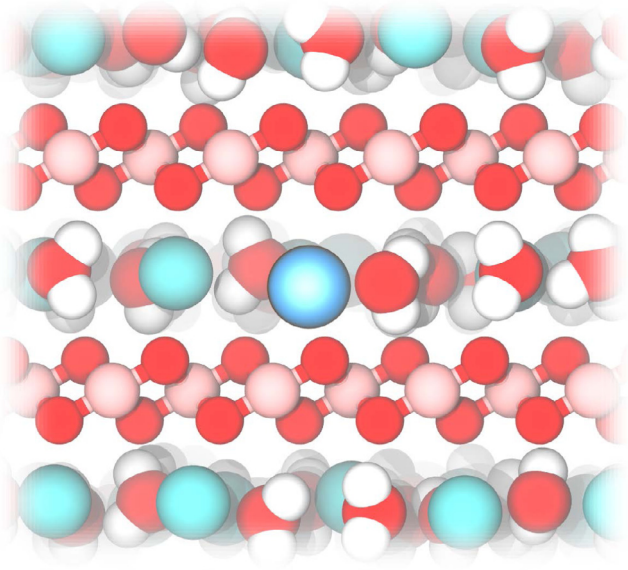

Fig. 1. Snapshot of the aqueous solution confined between the layered MnO_2 sheets of birnessite. Oxygen atoms are colored red, hydrogen atoms are white, manganese are colored pink, and potassium ions are green. The redox active ion undergoing a change in charge state (M) is indicated by the blue sphere near the center of the figure. Some molecules have been omitted for clarity. (For interpretation of the references to colour in this figure legend, the reader is referred to the web version of this article.)

2. Non-equilibrium relaxation dynamics in response to charge transfer are non-linear

We characterize the nonequilibrium relaxation dynamics of the system through the response function [29,30]

$$S(t) = \frac{\overline{\Delta E}(t) - \overline{\Delta E}(\infty)}{\overline{\Delta E}(0) - \overline{\Delta E}(\infty)}, \tag{1}$$

where $\overline{F}(t)$ indicates a nonequilibrium average of an observable $F(t)$ over trajectories propagated with the solute in its excited (oxidized) state, but prepared with initial states sampled from the Boltzmann distribution corresponding to the ground (reduced) state. Here, the ground state of the model redox ion (blue in Fig. 1) corresponds to a charge of $q = +1$, such that the ion is equivalent to all others in the system. The excited state is obtained when $q = +2$, where the negative charge has transferred to the nearest Mn site, following previous work [8]. The nonequilibrium averages were computed over 70 initial configurations with 20 trajectories per configuration, each initialized with randomized velocity distributions. Here, $\Delta E(t) \equiv \Delta E(\overline{\mathbf{R}}(t))$ is the energy gap between the ground and excited states [9,13,29–32], defined as the difference between the respective Hamiltonians $\mathcal{H}_0$ and $\mathcal{H}_1$ in configuration $\overline{\mathbf{R}}(t)$ at time t,

$$\Delta E(\overline{\mathbf{R}}(t)) = \mathcal{H}_1(\overline{\mathbf{R}}(t)) - \mathcal{H}_0(\overline{\mathbf{R}}(t)), \tag{2}$$

where $\mathcal{H}_\lambda$ is in general the Hamiltonian of state λ.

If the system responds linearly, the nonequilibrium correlation function $S(t)$ is equal to the equilibrium time correlation function of the energy gap [29,30],

$$C_\lambda(t) = \frac{\langle \delta\Delta E(t)\delta\Delta E(0)\rangle_\lambda}{\left\langle (\delta\Delta E(0))^2 \right\rangle_\lambda}, \tag{3}$$

where $\langle F\rangle_\lambda$ indicates an equilibrium ensemble average of F over configurations sampled under the Hamiltonian $\mathcal{H}_\lambda$, and $\delta\Delta E(t) = \Delta E(t) - \langle \Delta E\rangle$. $C_\lambda(t)$ was computed by averaging over the results obtained from 16 trajectories with independent initial conditions taken from an equilibrium simulation 100 ns in duration. Each trajectory in the $\lambda = 1$ state was equilibrated for at least an additional 10 ns before computing $C_1(t)$. This averaging over initial conditions is necessary because of the slow dynamics in this system.

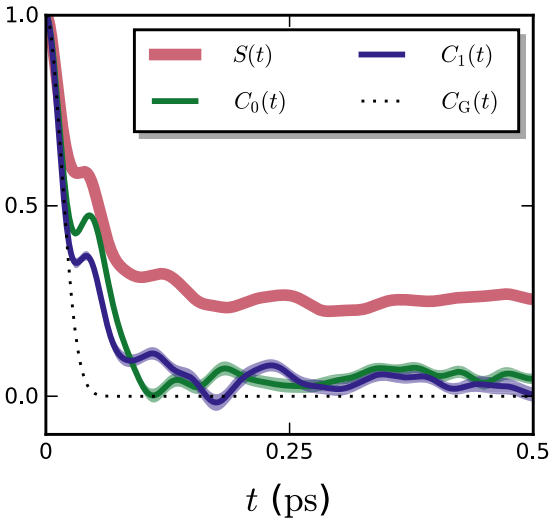

Fig. 2. The nonequilibrium response function does not equal its equilibrium counterparts even approximately, $S(t) \neq C_\lambda(t)$, respectively. Shaded regions indicate one standard error.

The above response functions are shown in Fig. 2 and illustrate that $S(t) \neq C_\lambda(t)$, although $C_1(t)$ more closely mimics the general features of $S(t)$. This is not surprising since both $S(t)$ and $C_1(t)$ are evolving in time under the same Hamiltonian, $\mathcal{H}_1$; similar conclusions have been drawn in simpler systems [33]. The violation of linear response theory illustrated in Fig. 2 is largely a result of a non-Gaussian free energy landscape underlying the charge transfer process. We note that non-stationarity of even Gaussian free energy landscapes under time evolution also contribute to violations of linear response theory [34].

We find that multiple timescales are involved in the decay of $S(t)$, the features of which can be traced to their molecular origins. This is now detailed below.

3. Molecular origins of non-linear relaxation

3.1. Relaxation dynamics are Gaussian at very short times

Despite the differences in the three correlation functions shown in Fig. 2, the initial rapid decay of $S(t)$ is captured equally well by both $C_0(t)$ and $C_1(t)$, suggesting Gaussian time character at short times governed by the inertial motion of solvent molecules [33,35–39], despite the total nonequilibrium response being non-Gaussian. Indeed, the Gaussian approximation to the dynamics $C_G(t)$ accurately captures the short-time relaxation behavior, as evidenced in Fig. 2, where

$$C_G(t) = e^{-\omega_\lambda^2 t^2/2} \tag{4}$$

and

$$\omega_\lambda^2 = \frac{\left\langle (\delta\Delta\dot{E})^2 \right\rangle_\lambda}{\left\langle (\delta\Delta E)^2 \right\rangle_\lambda}, \tag{5}$$

such that the dot indicates a time derivative and the ensemble averages can be performed over either end point. We find $\omega_0 = 62 \pm 15$ ps^{-1} and $\omega_1 = 68 \pm 17$ ps^{-1}, where the error bars represent the standard error between the trajectories averaged to

obtain ω. Because $\omega_0 \approx \omega_1, C_G(t)$ is nearly identical for both end states, in agreement with the initial decays of $C_0(t)$ and $C_1(t)$.

3.2. Local orientational response creates initial deviations from Gaussianity

The Gaussian relaxation at short times is dominated by inertial effects and determines the smallest relaxation time. On picosecond timescales, the relaxation is bimodal, and the relaxation on intermediate times does not result from such inertial effects. Instead, this relaxation time is dictated by the response of the solvent, and water in particular.

We find that the short-time response to charge transfer is dominated by the local response of water molecules in the hydration shell of the charge transfer site. This local orientational response of hydration shell water molecules can be quantified by the response function

$$S_{DK}(t) = \frac{\overline{\cos\theta_{DK}}(t) - \overline{\cos\theta_{DK}}(\infty)}{\overline{\cos\theta_{DK}}(0) - \overline{\cos\theta_{DK}}(\infty)}. \quad (6)$$

Here, θ_{DK} is the angle that the dipole moment of a water molecule makes with the vector connecting that water's oxygen site to the center of the charge transfer ion, averaged over the three water molecules closest to the ion.

As shown in Fig. 3, the initial Gaussian short-time decay of $S(t)$ is not quantitatively described by $S_{DK}(t)$, because the latter correlation function does not quantify translational relaxation processes, although the initial relaxation time is captured. The qualitative features of $S(t)$ on these time-scales are mirrored by those of $S_{DK}(t)$; oscillations in both functions are in phase. This suggests that the subpicosecond behavior of $S(t)$ is dominated by the local relaxation of water molecules in the hydration shell of the charge transfer species. Longer-ranged reorganizations involving water and ions outside of the first hydration shell may have a minor role in this short-time process, but their dominant contribution is to the long-time relaxation of $S(t)$.

3.3. Slow and collective translational dynamics govern intermediate to long time response

As a measure of the translational solvation dynamics, we monitor the relaxation of the number of the water oxygen atoms N_O in the hydration shell of the redox ion through the correlation function

$$S_{N_O}(t) = \frac{\overline{N_O}(t) - \overline{N_O}(\infty)}{\overline{N_O}(0) - \overline{N_O}(\infty)}. \quad (7)$$

Here, the coordination number $N_O(t)$ is defined as the number of oxygen atoms within 0.3 nm of the ion, which is the location of the first minimum in the ion-water pair correlation function with the ion in its oxidized state. The coordination structure of the ion significantly differs between the end states, with $\langle N_O\rangle_0 \approx 3$ and $\langle N_O\rangle_1 \approx 4$, evidenced by the pair density distribution functions shown in Fig. 4. Moreover, the change in water coordination is accompanied by expulsion of ions from the coordination shell due to the increase in ionic charge-charge repulsions and dipole-charge repulsions induced by the orientational ordering of water molecules.

On a timescale on the order of 1 ps, the sudden change in ionic charge simply pulls nearby waters closer, and the relaxation of $S_{N_O}(t)$ closely follows that of $S(t)$, indicating that this local change in coordination number determines the relaxation behavior on this timescale. However, both $S_{N_O}(t)$ and $S(t)$ do not fully relax on this timescale, and the coordination number has not yet reached that of the fully equilibrated end state. We anticipate that complex

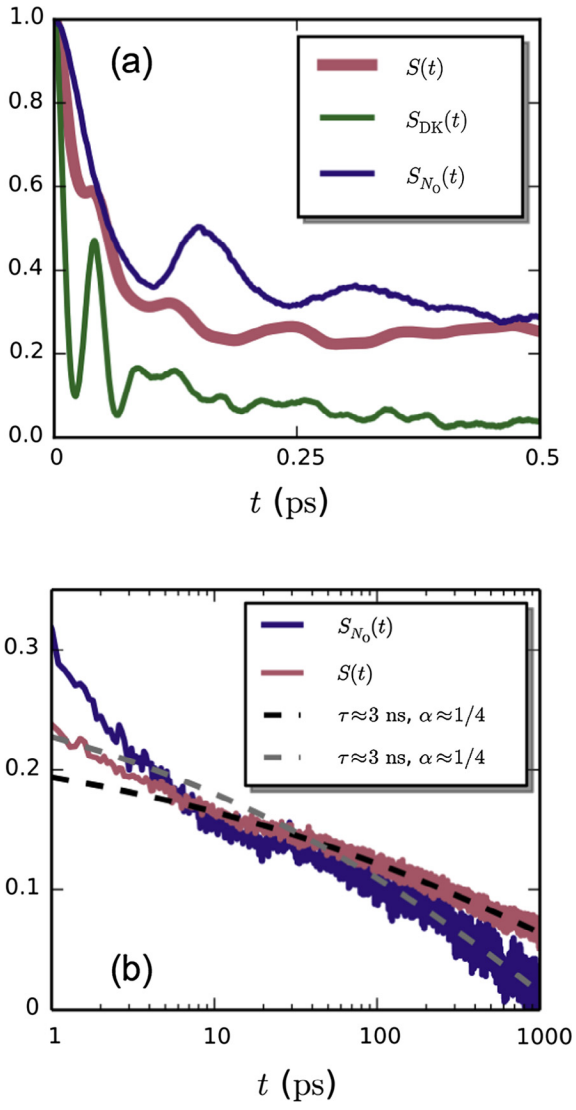

Fig. 3. The salient features of the nonequilibrium energy gap response function $S(t)$ agree well with those of the nonequilibrium response function characterizating the orientational relaxation of water in ion hydration shells, $S_{DK}(t)$, indicating that the local reorientation of hydration waters underpins the nature of solvation dynamics at short times. At longer times, solvation dynamics are dominated by slow translational dynamics, exemplified by the coordination number response function $S_{N_O}(t)$. Data in panel (a) for 1 ps trajectories is obtained with higher resolution than the 1 ns in panel (b). Dashed lines in (b) are fits to stretched exponential functions.

rearrangements of the hydration shell must occur for the system to fully relax. These rearrangements require translation of atoms in the complex environment of the interlayer that occur on timescales longer than water reorientation.

Indeed, the longest relaxation time of $S(t)$, τ, coincides with the long-time decay of $S_{N_O}(t)$, as shown in Fig. 3. Moreover, the long-time relaxation is consistent with a stretched exponential form, indicative of collective dynamics reminiscent of glassy systems [40–42]. We have also observed other signatures in the interlayer that suggest cooperativity in the dynamics of confined water and ions, and this is to be detailed in a forthcoming publication. A fit of the long-time behavior of $S(t)$ to the stretched exponential [40,41]

$$f(t) = f_0 + f_1 e^{-(t/\tau)^\alpha} \quad (8)$$

yields $\tau = 2999$ ps, in agreement with a similar fitting of $S_{N_O}(t)$, yielding $\tau = 3000$ ps, both with $\alpha = 0.24$; the parameters f_0 and f_1

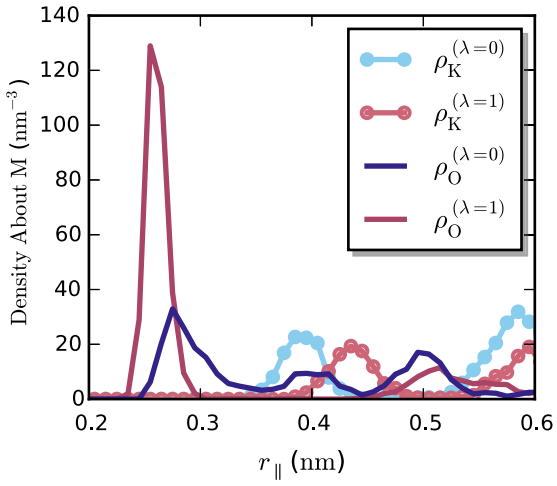

Fig. 4. In plane pair densities for potassium ions (K) and oxygen sites (O) around the model redox active ion (M) in the reduced ($\lambda = 0$) and oxidized ($\lambda = 1$) states. The first peak in the oxygen density moves to smaller distances and significantly increases in height upon oxidation, while the K^+ peak moves to larger distances, indicating exchange of ions for water in the hydration shell of the redox ion. The distance in the two-dimensional plane is indicated by $r_{\parallel}$.

vary between the two fits. Thus, we conclude that the slowest relaxation time τ in response to charge transfer corresponds mainly to the dynamics surrounding an increase in the ion coordination number, and the timescale for this increase in coordination number is set by the collective dynamics required to translate a fourth water molecule into the ion hydration shell.

4. Conclusions

In this work, we have characterized the response of water and ions in the interlayer of birnessite to a charge transfer event, wherein a single ion is oxidized by undergoing electron transfer with the MnO_2 surface. Understanding the molecular details surrounding electron transfer and similar events in this and analogous materials is critical to understand their utility in catalytic applications.

Knowledge of the nature of water relaxation in response to charge transfer events will aid in future studies of the mechanism of water oxidation in birnessite. We find that the non-linear relaxation proceeds on three time-scales. The first is Gaussian and governed by inertial response that is not unique to this system or process. The second timescale is controlled by local structural rearrangements of the ionic hydration shell, namely water reorientation and translation within the coordination shell, without significant changes in coordination number. A key finding is that there exists a third, much longer relaxation time on the order of several nanoseconds that accompanies a change in coordination number of the redox species. This relaxation process arises from slow, collective dynamics in the system that facilitate the movement of water and ions within the interlayer and is similar in spirit to what is observed in glassy systems [40–42] and at complex interfaces with tightly bound waters [43,44].

The slow relaxation time arising from collective dynamics is important in understanding reaction mechanisms and overall chemical dynamics in this material. As an example, consider the following simple two-step reaction in birnessite: (i) an electron is transferred from an ion to the surface and (ii) this induces bond breaking in a nearby molecule. If step (ii) occurs within a few nanoseconds after step (i), the system may not be in equilibrium, even locally. In fact, because the relaxation process is closely tied to structural rearrangements, the solvation structure around the redox site may be substantially different from what one would expect at equilibrium. Thus, any study of such reaction mechanisms and their associated thermodynamics should account for the possible nonequilibrium structures and associated fields in this system.

5. Simulation details

Following our previous work [8], simulations were performed with the GROMACS5 software package [45], and the CLAYFF force field [46] was used to describe the the K^+ ions and transition metal oxide surface, modified to include Mn interaction potentials [47]. The MnO_2 sheets were held fixed in their crystal structure [7,6], although the distance between the sheets was set to the equilibrium value determined previously for the CLAYFF parameters [47]. We mimicked an open system by leaving the edges of the birnessite along one axis open to water reservoirs, which were kept in equilibrium with vapor. This allows the system to be held at a constant pressure equal to that at water-vapor coexistence. All simulations were performed in the canonical ensemble (constant NVT), with the temperature maintained at $T = 300$ K using the canonical velocity-rescaling thermostat of Bussi et al. [48]. Water was modeled using the extended simple point charge model (SPC/E) [49], in accord with the parameterization of CLAYFF [46].

Acknowledgements

This work was supported as part of the Center for the Computational Design of Functional Layered Materials, an Energy Frontier Research Center funded by the U.S. Department of Energy, Office of Science, Basic Energy Sciences under Award #DE-SC0012575. We thank S. Balasubramanian and Hemant Kashyap for insightful discussions.

References

[1] C.E. Frey, M. Wiechen, P. Kurz, Water-oxidation catalysis by synthetic manganese oxides–systematic variations of the calcium birnessite theme, Dalton Trans. 43 (11) (2014) 4370–4379.
[2] I.G. McKendry, S.K. Kondaveeti, S.L. Shumlas, D.R. Strongin, M.J. Zdilla, Decoration of the layered manganese oxide birnessite with Mn(II/III) gives a new water oxidation catalyst with fifty-fold turnover number enhancement, Dalton Trans. 44 (29) (2015) 12981–12984.
[3] A.C. Thenuwara et al., Copper-intercalated birnessite as a water oxidation catalyst, Langmuir 31 (46) (2015) 12807–12813.
[4] A.C. Thenuwara et al., Nickel confined in the interlayer region of birnessite: an active electrocatalyst for water oxidation, Angew. Chem. Int. Ed. Engl. 55 (35) (2016) 10381–10385.
[5] C.L. Lopano, P.J. Heaney, J.E. Post, J. Hanson, S. Komarneni, Time-resolved structural analysis of K- and Ba-exchange reactions with synthetic Na-birnessite using synchrotron x-ray diffraction, Am. Mineral. 92 (2007) 380–387.
[6] B. Lanson, V.A. Drits, Q. Feng, A. Manceau, Structure of synthetic Na-birnessite: evidence for a triclinic one-layer unit cell, Am. Mineral. 87 (2002) 1662–1671.
[7] J.E. Post, D.R. Veblen, Crystal structure determinations of synthetic sodium, magnesium, and potassium birnessite using TEM and the Rietveld method, Am. Mineral. 75 (1990) 477–489.
[8] R.C. Remsing, I.G. McKendry, D.R. Strongin, M.L. Klein, M.J. Zdilla, Frustrated solvation structures can enhance electron transfer rates, J. Phys. Chem. Lett. 6 (23) (2015) 4804–4808.
[9] R.A. Marcus, Electron transfer reactions in chemistry. theory and experiment, Rev. Mod. Phys. 65 (3) (1993) 599–610.
[10] J.T. Hynes, Chemical reaction dynamics in solution, Annu. Rev. Phys. Chem. 36 (1985) 573–597.
[11] B. Bagchi, Dynamics of solvation and charge transfer reactions in dipolar liquids, Annu. Rev. Phys. Chem. 40 (1989) 115–141.
[12] A.H. Zewail, Femtochemistry: recent progress in studies of dynamics and control of reactions and their transition states, J. Phys. Chem. 100 (1996) 12701–12724.
[13] R.M. Stratt, M. Maroncelli, Nonreactive dynamics in solution: the emerging molecular view of solvation dynamics and vibrational relaxation, J. Phys. Chem. 100 (1996) 12981–12996.
[14] G.A. Voth, R.M. Hochstrasser, Transition state dynamics and relaxation processes in solutions: a frontier of physical chemistry, J. Phys. Chem. 100 (1996) 13034–13049.

[15] A.J. Orr-Ewing, Dynamics of bimolecular reactions in solution, Annu. Rev. Phys. Chem. 66 (2015) 119–141.
[16] D. Zhong, A. Douhal, A.H. Zewail, Femtosecond studies of protein-ligand hydrophobic binding and dynamics: human serum albumin, Proc. Natl. Acad. Sci. USA 97 (26) (2000) 14056–14061.
[17] K. Bhattacharyya, B. Bagchi, Slow dynamics of constrained water in complex geometries, J. Phys. Chem. A 104 (2000) 10603–10613.
[18] N.E. Levinger, Water in confinement, Science 298 (2002) 1722–1723.
[19] M.D. Fayer, N.E. Levinger, Analysis of water in confined geometries and at interfaces, Annu. Rev. Anal. Chem. (Palo Alto Calif) 3 (2010) 89–107.
[20] W.H. Thompson, Solvation dynamics and proton transfer in nanoconfined liquids, Annu. Rev. Phys. Chem. 62 (2011) 599–619.
[21] D. Zimdars, J.I. Dadap, K.B. Eisenthal, T.F. Heinz, Femtosecond dynamics of solvation at the air/water interface, Chem. Phys. Lett. 301 (1999) 112–120.
[22] D. Pant, N.E. Levinger, Polar solvation dynamics of H_2O and D_2O at the surface of zirconia nanoparticles, J. Phys. Chem. B 103 (1999) 7846–7852.
[23] S. Balasubramanian, B. Bagchi, Slow solvation dynamics near an aqueous micellar surface, J. Phys. Chem. B 105 (2001) 12529–12533.
[24] S.K. Pal, J. Peon, A.H. Zewail, Biological water at the protein surface: dynamical solvation probed directly with femtosecond resolution, Proc. Natl. Acad. Sci. USA 99 (4) (2002) 1763–1768.
[25] S.K. Pal, A.H. Zewail, Dynamics of water in biological recognition, Chem. Rev. 104 (2004) 2099–2123.
[26] L.R. Martins, M.S. Skaf, B.M. Ladanyi, Solvation dynamics at the water/zirconia interface: molecular dynamics simulations, J. Phys. Chem. B 108 (2004) 19687–19697.
[27] I. Benjamin, Solute dynamics at aqueous interfaces, Chem. Phys. Lett. 469 (2009) 229–241.
[28] I. Benjamin, Reaction dynamics at liquid interfaces, Annu. Rev. Phys. Chem. 66 (2015) 165–188.
[29] B. Bagchi, Molecular Relaxation in Liquids, Oxford University Press, New York, 2012.
[30] A. Nitzan, Chemical Dynamics in Condensed Phases: Relaxation, Transfer, and Reactions in Condensed Molecular Systems, Oxford University Press, New York, 2006.
[31] J. Blumberger, I. Tavernelli, M.L. Klein, M. Sprik, Diabatic free energy curves and coordination fluctuations for the aqueous Ag + Ag^{2+} redox couple: a biased Born-Oppenheimer molecular dynamics investigation, J. Chem. Phys. 124 (6) (2006) 64507.
[32] R. Ayala, M. Sprik, A classical point charge model study of system size dependence of oxidation and reorganization free energies in aqueous solution, J. Phys. Chem. B 112 (2008) 257–269.
[33] E.A. Carter, J.T. Hynes, Solvation dynamics for an ion pair in a polar solvent: time-dependent fluorescence and photochemical charge transfer, J. Chem. Phys. 95 (1991) 5961–5979.
[34] P.L. Geissler, D. Chandler, Importance sampling and theory of nonequilibrium solvation dynamics in water, J. Chem. Phys. 113 (2000) 9759–9765.
[35] M. Maroncelli, G.R. Fleming, Computer simulation of the dynamics of aqueous solvation, J. Chem. Phys. 89 (1988) 5044–5069.
[36] R. Jimenez, G.R. Fleming, P.V. Kumar, M. Maroncelli, Femtosecond solvation dynamics of water, Nature 369 (1994) 471–473.
[37] B.M. Ladanyi, M.S. Skaf, Computer simulation of hydrogen-bonding liquids, Annu. Rev. Phys. Chem. 44 (1993) 335–368.
[38] B.M. Ladanyi, R.M. Stratt, Short-time dynamics of solvation: linear solvation theory for polar solvents, J. Phys. Chem. 99 (1995) 2502–2511.
[39] D. Laage, G. Stirnemann, F. Sterpone, R. Rey, J.T. Hynes, Reorientation and allied dynamics in water and aqueous solutions, Annu. Rev. Phys. Chem. 62 (2011) 395–416.
[40] M.D. Ediger, C.A. Angell, S.R. Nagel, Supercooled liquids and glasses, J. Phys. Chem. 100 (1996) 13200–13212.
[41] D. Roy, M. Maroncelli, Simulations of solvation and solvation dynamics in an idealized ionic liquid model, J. Phys. Chem. B 116 (2012) 5951–5970.
[42] D. Chandler, J.P. Garrahan, Dynamics on the way to forming glass: bubbles in space-time, Annu. Rev. Phys. Chem. 61 (2010) 191–217.
[43] D.T. Limmer, A.P. Willard, P. Madden, D. Chandler, Hydration of metal surfaces can be dynamically heterogeneous and hydrophobic, Proc. Natl. Acad. Sci. USA 110 (11) (2013) 4200–4205.
[44] A.P. Willard, D.T. Limmer, P.A. Madden, D. Chandler, Characterizing heterogeneous dynamics at hydrated electrode surfaces, J. Chem. Phys. 138 (18) (2013) 184702.
[45] B. Hess, C. Kutzner, D. van der Spoel, E. Lindahl, Gromacs 4: algorithms for highly efficient, load-balanced, and scalable molecular simulation, J. Chem. Theory Comp. (2008) 435–447.
[46] R.T. Cygan, J.-J. Liang, A.G. Kalinichev, Molecular models of hydroxide, oxyhydroxide, and clay phases and the development of a general force field, J. Phys. Chem. B 108 (2004) 1255–1266.
[47] R.T. Cygan, J.E. Post, P.J. Heaney, J.D. Kubicki, Molecular models of birnessite and related hydrated layered minerals, Am. Mineral. 97 (2012) 1505–1514.
[48] G. Bussi, D. Donadio, M. Parrinello, Canonical sampling through velocity rescaling, J. Chem. Phys. 126 (1) (2007) 014101.
[49] H.J.C. Berendsen, J.R. Grigera, T.P. Straatsma, The missing term in effective pair potentials, J. Phys. Chem. 91 (1987) 6269–6271.